8-2017

Characterization of a Tuberous Sclerosis Complex 2 Variant and its Interaction Involving the Ras-Related Protein Rheb

Nosaiba Shokr
University of Arkansas, Fayetteville

Characterization of a Tuberous Sclerosis Complex 2 Variant and its Interaction Involving the Ras-Related Protein Rheb

A thesis submitted in partial fulfillment
of the requirements for the degree of
Master of Science in Cell and Molecular Biology

by

Nosaiba Shokr
King Abdul-Aziz University
Bachelor of Science in Medical Laboratory Technology, 2011

August 2017
University of Arkansas

This thesis is approved for recommendation to the Graduate Council

_____
Dr. Paul Adams
Thesis Director

_____
Dr. Josh Sakon
Committee Member

_____
Dr. Mack Ivey
Committee Member

Abstract

Structure-function relationships of any complex underlie the molecular details of the biological interactions. Rheb, Ras Homology Enriched in Brain, is a Ras-related protein, and it is genetically identified as a molecular switch. Rheb is regulated by cycling between the biologically active GTP and inactive GDP-bound forms. This regulation is partially controlled by an interaction with Tuberous Sclerosis Complex2 (TSC2), a GTPase activating protein (GAP). Upon interaction, TSC2 stimulates Rheb GTP hydrolysis and diminishes the mammalian target of rapamycin (mTOR) pathway. The mTOR pathway is involved in proteins synthesis, cell cycle, and signaling. Mutation in TSC2 causes abnormal activation of Rheb and affects the mTOR pathway signaling. However, the molecular details of this interaction are still largely unidentified. The goal of this project is to characterize the molecular features of TSC2-218-N119K interaction by using biochemical and biophysical methods. The long-term objectives are to fill the gap in understanding TSC2-Rheb interaction, TSC2 GAP mechanism, and how that affects the mTOR pathway.

Acknowledgment

I am deeply grateful to my adviser Paul Adams (Associate Professor in Biochemistry at the University of Arkansas). His guidance, encouragement, and supervision from the first step to the last have allowed me to complete this project. I will always remember him saying that there is no right or wrong answer but the most important thing that you think critically.

My appreciation goes to the committee members: Dr. Mack Ivey (Associate Professor in Biological sciences at the University of Arkansas) and Dr. Josh Sakon (Professor in Biochemistry at the University of Arkansas) for their valuable time and efforts. I would like also to express my gratitude to my lab colleagues. Without their kindness, support, and motivation this project could not be done. I extend my thanks to my country who granted me this generous scholarship.

Finally, my prime motivation behind this research project are my family and friends. I have had a dream of pursuing my education abroad and my parents made it possible. Even though I was busy most of the time, my family and friends never forgot sharing me my birthdays and the happy holidays.

Contents

Introduction

1.1 mTOR Pathway

Organisms grow when cells receive proper signals for metabolic activity. In order to achieve balance between anabolism and catabolism processes, signals must be regulated to ensure that the cells perform their proper functions. Dysregulation of the signaling pathways leads to homeostasis disruption and disease occurrence. The mammalian serine/threonine protein kinase target of rapamycin mTOR pathway plays a significant role in cell synthesis, proliferation, and autophagy[1]. Dysregulation of the mTOR pathway has been reported to cause several health issues such as cancer and metabolic diseases[2].

There are two complexes in the mTOR pathway which are mTOR complex1 (mTORC1) and mTOR complex 2 (mTORC2) and each one of them integrates with different components and stimuli[1]. The major components of mTROC1 are regulatory-associated proteins of mTOR (RAPTOR), and mammalian lethal with SEC thirteen 8 (mLST8)[1]. Activation of mTORC1 promotes protein synthesis and initiates translation by phosphorylating ribosomal protein S6 (S6K1) and eIf4E-binding protein, respectively (4E-BP)[3,4]. In addition, it enhances the pentose phosphate pathway genes expression and therefore increases 5′-phosphoribosyl-1'-pyrophosphate (PRPP) production, which is the building block of purine and pyrimidine nucleotides[2]. The mTORC1 pathway promotes lipogenesis through activation of the major regulators of lipid biosynthesis (SREBPs) and inhibition of the phosphatidic acid phosphatase that obstructs SREBPs function (LIPIN1)[2]. Moreover, it controls autophagy, a process of cell destruction, through multiple ways including phosphorylation of UNC-51-like kinase1 that binds to 5' adenosine monophosphate -activated protein kinase and inhibits autophagy[5]. The mTORC1 pathway is initially activated in response to different stimuli such as

nutrients, growth factors or high cellular energy[6]. These signals are transmitted to mTORC1 through the regulation of a small G-protein called Rheb, which is a direct essential activator located upstream of mTORC1.

1.2 Rheb

Ras homology enriched in brain (Rheb) is a small GTPase protein that belongs to the Ras superfamily of G-proteins. The main function of Rheb is to control cell metabolism, growth, and proliferation through the mTORC1 cascade[7]. Rheb is predominantly in an active state in the cell, unlike the most of Ras GTPases, because of Rheb's low intrinsic GTPase activity and the small quantity TSC complex[8]. The structure of Rheb exhibits high similarity, 30-40% sequence identity, to other Ras proteins[9]. Rheb possess several characteristics that are different from other Ras proteins. For instance, during GTP/GDP exchange, Rheb switch II region retains a stable confirmation change whereas the long α-helical conformation occurs in Ras proteins[9]. Rheb switch I region constitutes residues from 33 to 41 (resembles 30-80 residues of Ras), and switch II region constitutes residues from 63 to 79 (resembles 60-76 residues of Ras) [9]. The existence of Gln64 in a deep hydrophobic core, instead of the surface like Gln61 in Ras proteins, makes it less accessible for GTP/GDP binding. Furthermore, unlike Tyr32 in Ras, the corresponding Tyr35 in Rheb shields the GTP phosphate moiety[9]. Lastly, Rheb possess arginine and serine residues in its P-loop that bind to the beta domain of GDP or GTP, instead of glycine residues like other Ras proteins[10]. Because of these differences, it has been suggested that Rheb has a unique GTPase mechanism. In fact, Asp65 in switch II and Thr38 in switch I are critical for Rheb GTP hydrolysis. However, Tyr35 residue in Rheb prevents the intrinsic GTPase catalytic activity by blocking the access of Asp65 to the nucleotide binding pocket[11].

Two mechanisms have been reported for activation of mTORC1 by Rheb. First, Liu *et al*. and Guo *et al*. claimed that peptidyl-prolyl-cis/trans-isomerase FKBP38 directly links Rheb to mTORC1. However, the findings of Wetzker *et al*. and Tang *et al*. studies contradict the previous claim[12–15]. Therefore, the mechanism of mTORC1 activation remains controversial. Second, indirect stimulation by phosphatidic acid (PA) has been confirmed after treating HEK293 cells with PA and measuring the phosphate level of the downstream substrates of the mTORC1, S6K1 and 4E-BP[16]. The active Rheb binds and activates phospholipase D1, which produces PA that can activate mTORC1[17].

The activity of Rheb can be regulated by Guanine nucleotide Exchange Factors (GEFs) and GTPase Activating Proteins (GAPs) (Figure 1). GEFs induce the release of bound GDP to be replaced by GTP and, therefore, activate the downstream substrates. However, GAPs catalyze the hydrolysis of bound GTP to the GDP and thereby switch off the downstream pathway[8]. The proteins that functions as GEFs are still unknown but the protein that acts as a GAP for Rheb is TSC2.

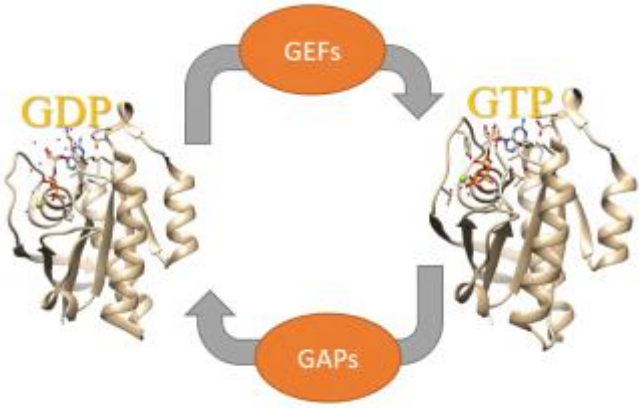

Figure 1. Rheb GDP/GTP cycle. GEFs phosphorylate Rheb and GAPs stimulate GTP hydrolysis. Rheb-GDP (1XTQ.pdb), Rheb-GTP (1XTS.pdb)[42].

1.3 TSC2

The inhibition of TSC2 GAP activity occurs when the cells receive the growth factor signals. Structural studies show that these signals leads to the phosphorylation of TSC2 on ser939, ser981, ser1130, ser1132 and thr1462[1]. As a result, Rheb becomes permanently loaded with GTP and, therefore, activates the rest of the mTORC1 pathway[1]. On the other hand, the absence of nutrients and the low energy level leads to the phosphorylation of TSC2 on ser1387 and that promotes the GAP catalytic activity toward Rheb[3]. Therefore, the now inactive GDP-Rheb inhibits phosphorylation of the mTORC1 substrates and stops cell growth and synthesis (Figure 2)[3].

TSC2 is active in a ternary complex with TSC1 and TBC1D7[18]. Aberrant function and mutation in the TSC complex genes lead to a genetic disorder called tuberous sclerosis. TSC1 encodes a protein called hamartin, 140-KD, and TSC2 encodes a protein called tuberin, 200-KD[19]. These proteins share little homology with each other and they bind to form a heterodimer with the recently discovered third subunit TBC1D7[20,18,21]. The molecular function of TBC1D7 is still unknown but it is hypothesized that it is required for GAP activity and that it stabilizes hamartin and tuberin dimerization and interaction[18,22]. The TSC complex is located in multiple organs such as the brain, kidney, lung and pancreas[23]. Previous studies have investigated the role of the TSC complex in the cell, primarily by studying these proteins in *Drosophila melanogaster*[24,25]. One study showed that a TSC1/2 heterodimer mutation in drosophila increased cell size, and successive experiments indicated that the TSC1/2 complex interacts with several proteins leading to inhibition of the mammalian target of rapamycin pathway[24,25]. On the other hand, phosphorylation on specific sites of TSC2 by protein kinase B (AKT) leads to the activation of the mTOR cascade[20]. Specifically, the C-terminal of TSC2 is homologous to the

corresponding region in GAP proteins and hydrolyses Rheb. The resemblance of TSC2 C-terminal to other GAP domains was first recognized when it was cloned in 1993. The C-terminal constitutes amino acid residues from 1517 to 1674 and it has a significant homology to human RAP1 GAP region[26].

There have been several identified mutations in TSC2 in Tuberous Sclerosis patients[26]. These mutations have been shown to occur in the GTPase activating region of the TSC2 protein[27]. The identification of the mutations and the study of protein interactions have shed light on TSC pathogenesis and have provided valuable information about the mTOR regulation. However, the mechanism of TSC2 GAP domain hydrolysis of Rheb is not completely understood. Characterizing the molecular details of TSC2 mutations in the GAP region should facilitate a greater understanding on the mechanism. The working hypothesis is that certain mutations on the TSC2 region will affect the Rheb interaction, and therefore alter the GTP hydrolysis, or show differences in its binding to Rheb.

This project focuses on studying one mutation in the TSC2 gap catalytic domain, N1643K (Asn1643Lys) (Figure 3). This mutation was first discovered as a de novo mutation in a TSC patient in 1997 by Sampson *et al*[28]. Our approach was to characterize the importance of the asparagine to lysine mutation on the structure-function relationship of TSC2 in its interaction with Rheb. Asparagine is a polar residue that is generally present on proteins' surfaces[29], and its typically interacts with other polar amino acids via hydrogen bonding with peptide backbones and contributing to proteins binding. Moreover, asparagine is frequently found at the end of alpha helices, as highlighted in Figure 2.[30]. On the other hand, lysine is a positive charged residue that possess an **ε**-amino group, and hence this study characterizing the effect of the amino group presence in the GAP catalytic domain[30].

It is believed that TSC2 uses an asparagine-thumb mechanism, instead of an arginine finger like other Ras GAP proteins, to stimulate GTP hydrolysis of Rheb. This observation was derived from RAP1 asparagine-thumb mechanism and it was confirmed in previous studies[31,32]. It is expected that this mutation will deactivate the TSC2 GAP activity and that deactivation could be due to loss of TSC2-Rheb binding or loss the GAP function. Another mutation that is located in the GAP binding domain is K1638A (Lys1638Ala), which has been investigated in Dr. Adams lab by a previous student. This K1638A mutation caused a weaker binding with Rheb, a loss of GAP activity and further resulted in Rheb remaining in a GTP-bound state [33]. Therefore, this study implies that other mutations next to asparagine have influenced the thumb mechanism. Detailed work on how theses mutations impact the TSC2 GAP catalytic domain will reveal new information on the TSC disease.

A small-truncated TSC2 with 218 amino acids has been used in this study to eliminate the challenges of the full TSC2 length, 1807 amino acids. In Quilliam *et al.*, the TSC2-C terminus that contains the GAP binding regions (965-1807 amino acids) was cloned and proved its binding to Rheb *in vitro*[34]. Marshall *et al*., have showed that TSC2 residues 1525 to 1742 exhibits the highest expression and stability[32]. Therefore, in this project, TSC2 1525-1742—called TSC2-218—have been used to investigate the role TSC2 binding domain and its binding to Rheb by applying biochemical and biophysical applications.

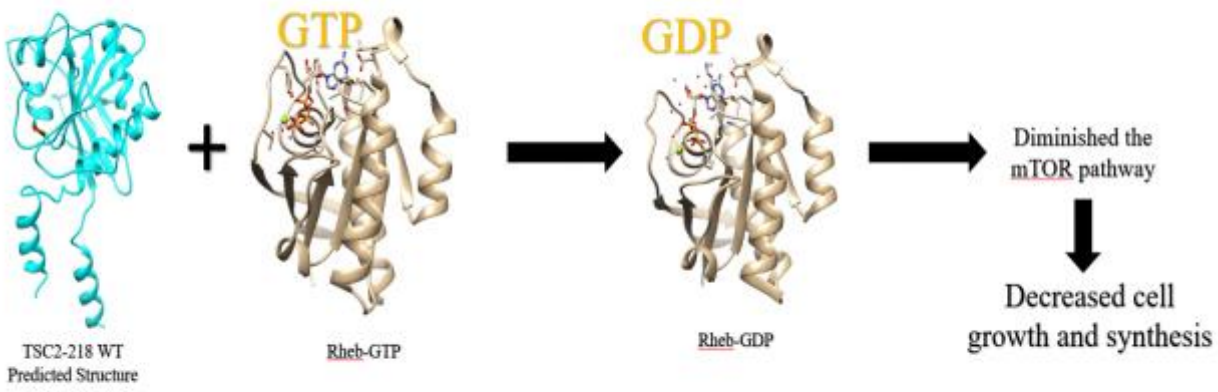

Figure 2. Representation of regular TSC2-Rheb activity. TSC2 dephosphorylates Rheb and Rheb-GDP decreases cell signaling. TSC2-218 predicted structure from I-TASSER, Rheb-GDP (1XTQ.pdb), Rheb-GTP (1XTS.pdb)[33,34,39]

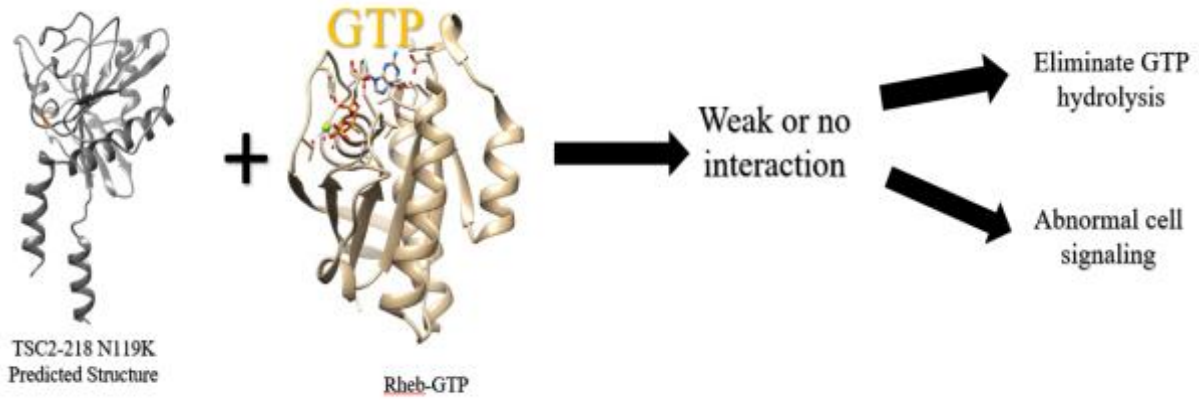

Figure 3. Representation of TSC2 N119K-Rheb activity. TSC2 could cause weak or no interaction and that leads to abnormal cell signaling. TSC2-218 N119K predicted structure from I-TASSER, Rheb-GDP (1XTQ.pdb), Rheb-GTP (1XTS.pdb) [33,34,39]

Materials and methods

2.1 Mutagenesis experiment

All plasmids were isolated using the QIAprep Spin Miniprep Kit protocol. First, 30 ml Luria-Bertani (LB) media, 30 μl ampicillin, and 500 μl glycerol stock were mixed in a 50ml tube and incubated overnight in a 37°C shaker. The next day, the tube was centrifuged for 15 minutes at 5000rpm. After that, the supernatant was discarded and the lysate was mixed with the buffers as instructed in the kit handbook. The concentration of the plasmid was determined using the UV-Vis at 260nm. The plasmid was sent along with the pGEX forward and reverse primers to the DNA Sequencing facility at the University of Arkansas for Medical Sciences for sequence verification. The primers for the TSC2-218 N119K were created using Quick Change Primer Design, an online tool. Several recommendations were taken into consideration when designing the primers[35]. The primer length was adequate to bind easily at a specific region. The primer melting temperature was less than 65°C to give the best result and to prevent the secondary annealing. In addition, the primer pairs had the same melting temperature to enhance efficiency and avoid mispriming. The GC content was acceptable to ensure stable binding between the primers and the template[35]. The forward and reverse primers were purchased from Integrated DNA Technologies. The primers were diluted first with elution buffer and then mixed with the PCR reaction buffers. The PCR mix reaction was created by adding 5μl of 10X reaction buffer, 1μl of TSC2-218 wild type plasmid, 1μl of forward and reverse primers, 1μl of dNTP mix, 3μl of Quick solution, 1μl of magnesium chloride (25mM), 39μl of sterile MQ water, and 1μl of pfu TURBO, DNA polymerase. PCR cycles were set to run according to Table 1.

Steps	Cycle	Temperature	Time	Cycle
1	1	95°C	1 minute	Initial denaturation
2	18		30 seconds	Denaturation
3		55°C	1 minute	Annealing
4		68°C	7 minutes	Elongation

Table 1: PCR Cycles conditions for site directed mutagenesis.

After the cycle was completed, 5µl of the product was set aside and labeled as undigested. 1.5µl of the restriction enzyme *DpnI* was added to the PCR product. The digested and undigested PCR amplified products, in addition to the DNA ladder, were loaded and run into the agarose gel. The gel image was taken using a transilluminator. After that, the DNA was transformed on NEB 5-alpha competent cells, which are highly efficient for transformation and isolation purposes. N119K DNA was added to the competent cells and incubated in ice for 30 minutes. The sample was heated and cooled for two minutes then added to 1ml of LB media. The sample was then incubated in the shaker at 37°C for two hours and later centrifuged for 10 minutes. 800µl was discarded and 100µl was plated into an LB agar inside the hood. The plate was incubated overnight at 37°C. Over the next day, 2-3 colonies were removed for plasmid isolation. Plasmid isolation was performed to confirm the variant's sequence. Once confirmed, the DNA was transformed into BL21 (DE3) cells, which are highly efficient for protein expression and harvesting.

2.2 Growth, harvesting, and purification

2.2A TSC2-218 Wild Type

A previous student performed test expressions and produced a standard protocol for obtaining TSC2-218 wild type, which was applied in this study[30]. Plasmid isolation was performed on BL21 (DE3), and colonies were transferred to 15mL LB media and 15μl ampicillin for a small-scale expression. Ampicillin was added to ensure that only bacteria that have incorporated the antibiotic resistant gene successfully in the plasmid will grow in the presence of the antibiotic. The mix was allowed to grow for 3-5 hours at 37°C in the shaker. After incubation, the tube was added to 100ml LB media with 100μl ampicillin and allowed to grow overnight in the 37°C shaker. The next day, the mixture was added to 1.5L LB media and 750μl ampicillin (large-scale expression). The optical density (OD) reading was taken using the UV-Vis at 600nm every hour until the reading reached to 0.8-1.0. This range is where the bacteria reach the mid-log phase (cells are set to produce the maximum number of proteins). Then, isopropyl β-D-1-thiogalactopyranoside (IPTG) was added to maximize the protein yield and was incubated for 5 hours at 25°C. After centrifugation, the precipitate was collected and resuspended with 10mM 1x phosphate buffered saline (PBS). After a 2nd centrifugation the collected pellet was either stored at -80°C or used directly for the purification. For the purification, the 1.5L pellet was thawed in ice and resuspended in the lysis buffer, which is 45ml 10mM 1x PBS buffer, 25mg lysozyme, Halt protease inhibitor cocktail, DNAse, and 25mM phenylmethane sulfonyl fluoride (PMSF). Sonication was applied to lyse the cell and free the proteins. The lysed cells were centrifuged at 29,000 rpm for 20 minutes and the supernatant was loaded on the fast protein liquid chromatography (FPLC) machine after it was filtered. For biding and elution buffers, 10mM PBS buffer pH7.3 and 0.02mM Tris HCL with 0.01mM fresh

glutathione pH8 were prepared, respectively. A glutathione S transferase (GST-tag) column was used to purify the protein. The column was cleaned first with guindium hydrochloride and guindium was removed with water. FPLC purification was accomplished in three steps. First, the column was equilibrated with the binding buffer. The target protein was then bound to the column through the tag and unbounded proteins were eluted. The last step was elution, where an isocratic gradient of the elution buffer was applied to elute the target protein in small fractions. The fractions were collected and gel electrophoresis was run in order to confirm the presence of the protein in the selected fractions. Once the target band was seen, the protein was dialyzed in 10mM PBS buffer pH7.3 overnight. The protein concentration was measured and thrombin was added accordingly, (where 1 unit thrombin can efficiently cleave 100μg protein). The protein and thrombin were incubated in a cold room for two hours. The GST-tag was removed by doing another FPLC purification. The fractions were collected and was run by SDS-PAGE to see the target band. The proteins were collected and dialyzed overnight and then lyophilized for long storage at -80°C or used directly for experiments.

TSC2-218 wild type predicted structure was generated based on the amino acid sequence of the C-terminal residues using 1-TASSER (an online tool that employs computational calculations to produce structure and function predications)[36]. Chimera was used to analyze the predicted structure and highlight the target residue for mutation[37].

2.2B TSC2-218 N119K

The isolation and purification protocol for TSC2-218 (N119K) was identical to the wild type. However, the protein aggregated after dialysis and before GST cleavage. An SDS-PAGE was performed to confirm the band of the precipitate and the supernatant. Next, an FPLC purification was applied for the supernatant using a GST-tag column to eliminate the cause of

aggregation. Several trials were attempted to prevent the aggregation including adding 10%glycerol and 25mM ammonium sulfate, incubating the protein at the cold room and room temperature, and exchanging the dialysis buffer each 3 hours. The aggregation was minimized when the pH of the dialysis buffer was increased to eight. The following purification steps and SDS-PAGE were performed the same as explained in the wild type section. TSC2-218 (N119K) predicted structure was generated as explained in the TSC2-218 wild type section.

2.2C Rheb

Rheb was overexpressed as a His_6-tag fusion protein and purified using a 5ml pre-packed Ni^{2+} column. The protein was tagged on the pET15b vector in *Escherichia coli* BL21 (DE3) strain. All cultures were induced with 0.5mM IPTG when the OD_{600} reached 0.6-0.8. Culture were then incubated for four hours in the shaker at 37°C. Centrifugation was applied to harvest the cells at 6,000 rpm for 20 minutes at 4°C. The pellet was resuspended in 10mM Tris pH 8 and was centrifuged at 5,000 rpm for 15 minutes at 4°C. For purification, the pellet was resuspended in the lysis buffer, which has Tris/HCl Ni^{2+} binding (pH 8.0, 01 M $MgCl_2$, 0.1 M NaCl, 0.05 Tris and 0.04 M imidazole) 45 mg lysozyme, halt protease, DNAse, and 25M PMSF. The cells were completely lysed using a sonicator with 12 short burst of 10 seconds followed by rest for 10 seconds and cooling for 4 minutes. Centrifugation was applied at 19,000rpm for 20 minutes at 4C° to remove cell debris. The supernatant was filtered and loaded on the FPLC machine to separate the target protein fractions. The binding buffer, Tris/Hcl Ni^{2+} binding (pH 8.0, 01 M $MgCl_2$, 0.1 M NaCl, 0.05 Tris and 0.04 M imidazole), and the elution buffer, Tris/Hcl Ni^{2+} binding (pH 8.0, 01 M $MgCl_2$, 0.1 M NaCl, 0.05 Tris and 0.25 M imidazole), were filtered before the purification was applied. The purification procedure was the same as stated before, but an increasing concentration of imidazole was achieved for protein elution. Next, an SDS-PAGE

was run to confirm the band size and purity. The collected protein fractions were dialyzed in 0.1 M NaCl, 0.02 M Tris, 0.01 M $MgCl_2$ pH8 at 4°C for overnight. For active Rheb, Rheb was nucleotide exchanged using a desalting PD-10 column. Rheb was incubated with 5mM GTP analog and 5mM EDTA for 1 hour at the cold room. The column was equilibrated with the binding buffer and then the protein was loaded into the column. The collected fractions were color tested by adding Bradford assay.10mM $MgCl_2$ was added to the dark blue color fractions. The protein could either be lyophilized or used directly for experiments.

2.3 Circular dichroism

Circular dichroism (CD) was carried out using a JASCO J-1500 CD Spectrometer to assess the protein secondary structure changes involving all TSC2-218 constructs, as well as protein interactions with Rheb were carried out. The Spectra Measurement program was used to collect the spectra in triplicate[38]. Purified proteins at a concentration of 0.1 mg/ml were suspended in 10mM 1x PBS buffer at pH7.3. The CD spectra were scanned between 250 and 190 nm in the 0.2 mm pathlength quartz spectrophotometer cell. The parameters were set to measure the spectra at 50 nm/min with accumulation of two scans for each spectrum, a spectral bandwidth of 1 nm, and a response time of 8 second. The data were expressed in molar ellipticity values according to equation 1,

$$Mollar\ Ellipticity = \frac{A}{C.M.L} \qquad \text{(Eq.1)}$$

where A is the absorbance, C is the concentration in g/L, M is the molecular weight in g/mol, and L is the pathlegnth of cell in cm. The final protein spectra were obtained by subtracting the buffer spectra, and the data were plotted using Origin.

CD difference spectra measurements were characterized by measuring the spectra of the incubated TSC2-218 wild type and TSC2-218(N119K) with the ligand protein, Rheb. The ligand spectra were subtracted from the ligand + protein spectra and the data were plotted using Origin.

2.4 Thermal denaturation:

Thermal denaturation experiments were performed using spectroscopy, as described earlier. The concentrations of the purified proteins were 0.2 mg/ml and they were suspended in 10 mM 1x PBS at pH7.3 in 0.2 mm pathlength quartz spectrophotometer cell. The temperature was set from 25 to 90 °C in steps of 0.5 °C/min and wavelength ranging from 190 to 250 nm. The midpoint temperature was monitored at a wavelength of 211 nm and was determined from the experimental sigmoid curve using Origin. Buffer spectra were measured and subtracted from each spectrum. Results were converted to molar ellipticity according to equation 1, and fraction of denatured protein was calculated according to equation 2,

$$Fd = \frac{MEx - MEi}{MEF - MEi} \qquad \text{(Eq.2)}$$

where F_d is the fraction of denatured protein, ME_x is the absorbance, ME_i is the fraction of the native protein, and ME_F is the fraction of the unfolded protein. Curves were created by plotting the fraction of denatured protein as a function of temperature.

2.5 Chemical denaturation

Chemical denaturation measurements were performed using CD also with 8M urea at 25°C. CD Spectroscopy was used because it is convenient and sensitive to protein 2° structure changes. The machine has an automatic titration function that spontaneously subtracts the protein of interest from the cuvette, and adds a specific quantity of denatured protein in high concentrations of urea. Then, the fluorescence measurement takes place after incubating the sample at a specified temperature. Data were collected using the automatic titration scan measurement

program, and the spectra were recorded in triplicate. 0.2 mg/ml of purified protein in 10mM phosphate buffer at pH 7.3 was titrated with urea in a 10mm pathlegnth cuvette. The cuvette has a stirrer bar in order to mix the solution with the titrant. Protein denaturation was monitored by measuring the fluorescence changes in the near-UV region (300-400 nm) with slits widths of 3 nm. Raw ellipticity values were converted to molar ellipticity using equation 1, and fractional denaturation was calculated according to equation 2 with applying fluorescence intensity instead of molar ellipticity intensity. Denaturation fractions were plotted as a function of urea concentration to determine denaturation midpoint values (Cm).

Results and discussion

3.1 Mutagenesis Study

The site directed mutagenesis was performed successfully and the DNA sequence was confirmed. To create the N119K construct, asparagine was replaced by lysing using the following primers: Forward: CGCGGTGGACCCGTTTCTGAAACACAGGTA Reverse: GCGCCACCTGGGCAAAGACTTTGTGTCCAT. Successful PCR amplification is shown in Figure 4. The bands in the first well are related to the molecular weight marker. The band in the lane 2 shows the undigested sample while the band in lane 3 indicates the amplified N119K. The amplified plasmid was transformed in two bacterial cell lines for isolation and expression. The transformation on BL21 (DE3) cells produced a good yield of colonies and it is shown in Figure 5.

3.2 Growth, harvesting, and purification:

TSC2 wild type or variant were grown and expressed as GST-tagged proteins. The proteins were purified using the FPLC machine—as described in the previous section—and SDS-PAGE was applied to ensure the proteins' purity. Figure 6 shows the TSC2-GST protein band after the first GST-tag chromatography purification. Lane 2 shows the lysate, which was collected before loading the sample into the machine. Lane 3 represents the flow through (unbound protein), which was collected after the protein binding on the column. It was expected that the protein band would be visible in the lysate and not in the flow through. This was confirmed, which indicated that the tagged protein was bound to the column. Lane 4, 5, 6 and 7 represent the GST-protein elution fractions. The band at 51 KDa is a combination of GST 26.9 KDa and TSC2-218 24 KDa as expected [(39)]. Figure 7a shows the SDS-PAGE after the second chromatography purification. Lane 2 shows the protein after incubating with thrombin. The

presence of two bands at 25 KDa indicate that the protein is cleaved from the GST tag. Lane 3,4,5, and 6 represent the pure TS2-218 fractions. The last two lanes show the GST bands at 25 KDa. The fractions were collected, dialyzed, and concentrated using a 10kDa MW cutoff Millipore centrifugal concentrator. The concentrated TSC2-218 band is shown in Figure 7b.

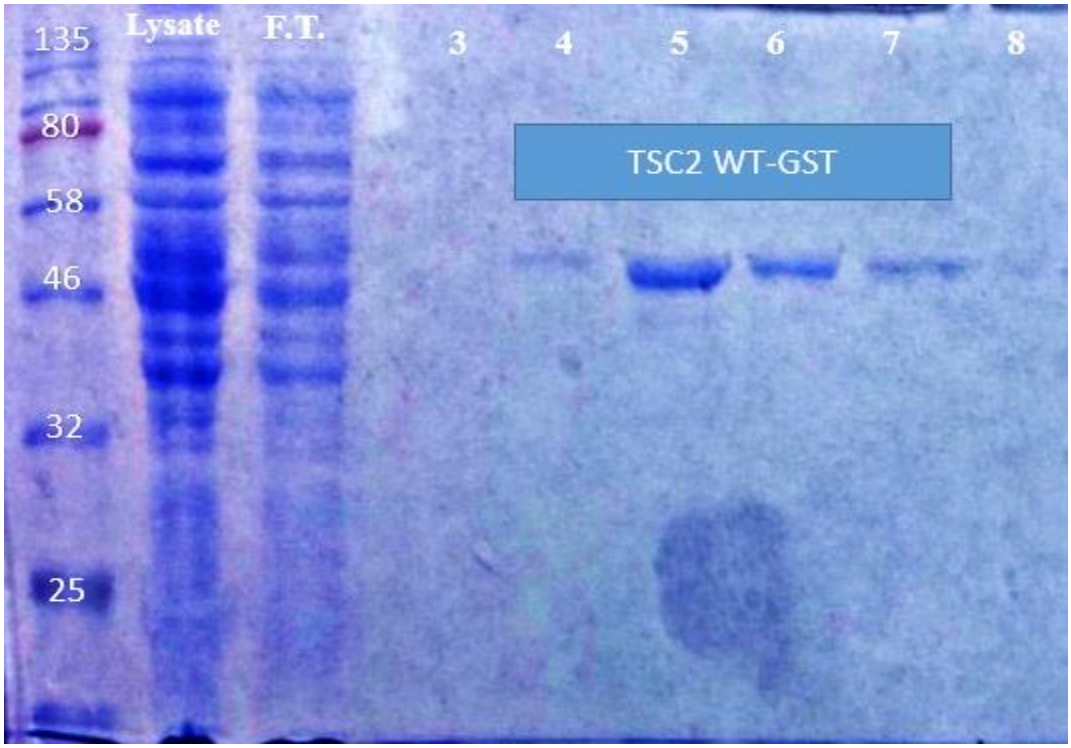

Figure 6: SDS-PAGE of the wild type protein after the first affinity purification. Lane 1 is the molecular weight marker. Lane 2 is the lysate. Lane 3 is the flow through. Lanes 4,5, 6, and 7 are different fractions of the TSC2-218-GST.

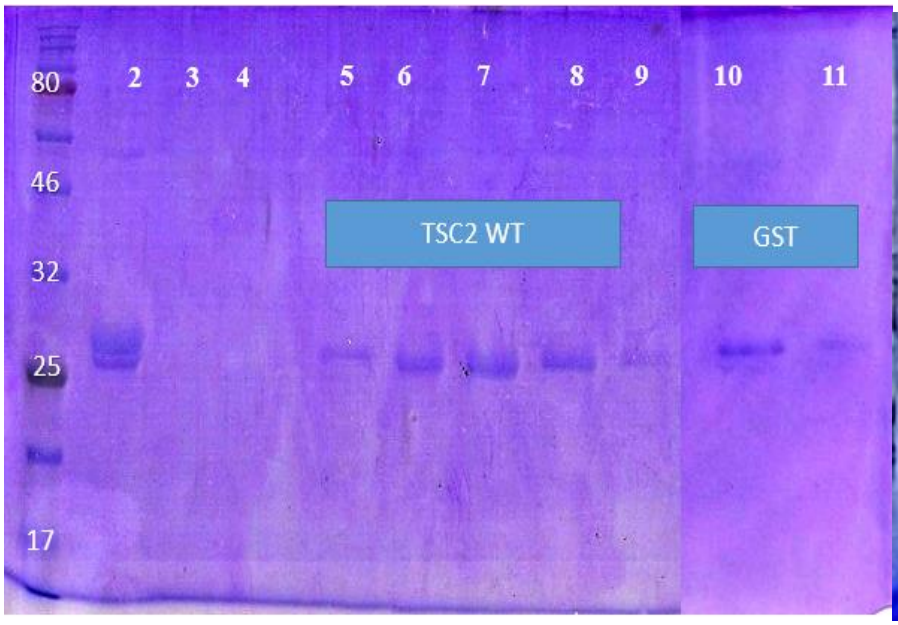

Figure 7a: SDS-PAGE of the wild type protein after the second affinity purification. Lane 1 is the molecular weight marker. Lane 2 is the cleaved protein. Lanes 5, 6,7,8, and 9 are different fractions of the TSC2-218. Lane 10 and 11 are GST bands.

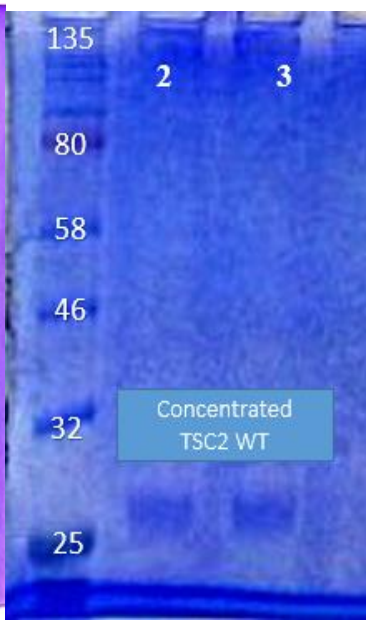

Figure 7b: SDS-PAGE of the concentrated TSC2-218 WT. Lane 1 is the molecular weight marker. Lane 2 and 3

For the TSC2-218 (N119K), Figure 8 shows the SDS-PAGE after the first chromatography purification. The TSC2-218 N119K-GST band is shown in the lysate and, with very low concentration, in the flow through, which indicates that most of the protein attached to the GST-column. Lane 5,6, 7, and 8 represent the TSC2-218 N119K-GST fractions. Another SDS-PAGE was performed to analyze the aggregation of the variant after the first successful purification and it is presented in Figure 9. Lane 2 shows the presence of intact N119K-GST sample before adding thrombin. Lane 3 represents the aggregation sample and it shows two bands: a higher intensity band at 51 KDa and a lower intensity band at 25 KDa. The higher intensity band indicates that most of the N119K-GST aggregated before cleavage occurrence.

Lane 4 contains the supernatant sample and shows a presence of a thick band at 25 KDa, which could be related to free GST or cleaved N119K. Another round of affinity chromatography purification was performed for the supernatant sample to determine if the band at 25 KDa is free GST or cleaved N119K, which confirmed the band was related to GST and demonstrated that the variant is more susceptible to aggregate. These observations led to test different dialysis environments in order to minimize the aggregation. Dialysis of the variant in 10mM 1x PBS pH 8 achieved the lowest aggregation occurrence. Figure 10a shows the SDS-PAGE after the second chromatography purification was applied. Lane 2 and 3 shows the cleaved N119k, and lanes 8-12 show the pure N119K fractions. The pooled protein fractions were dialyzed and concentrated using the same method as the wild type. The TSC2-218 (N119K) concentrated band is shown in Figure 10b.

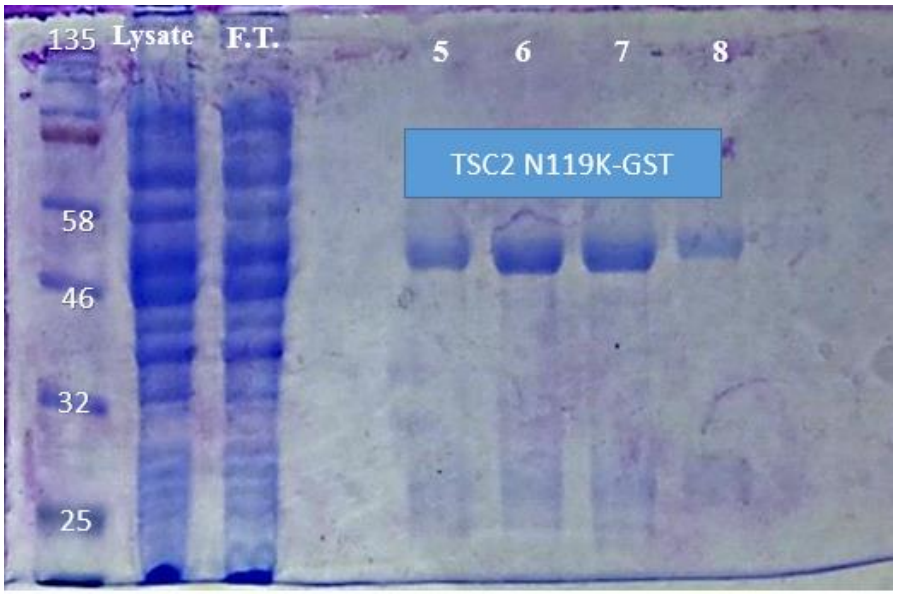

Figure 8: SDS-PAGE of TSC2-218-N119K after the first affinity purification. Lane 1 is the molecular weight marker. Lane 2 is the lysate. Lane 3 is the flow through. Lanes 5, 6, 7, and 8 are different fractions of the TSC2-218-N119K-GST.

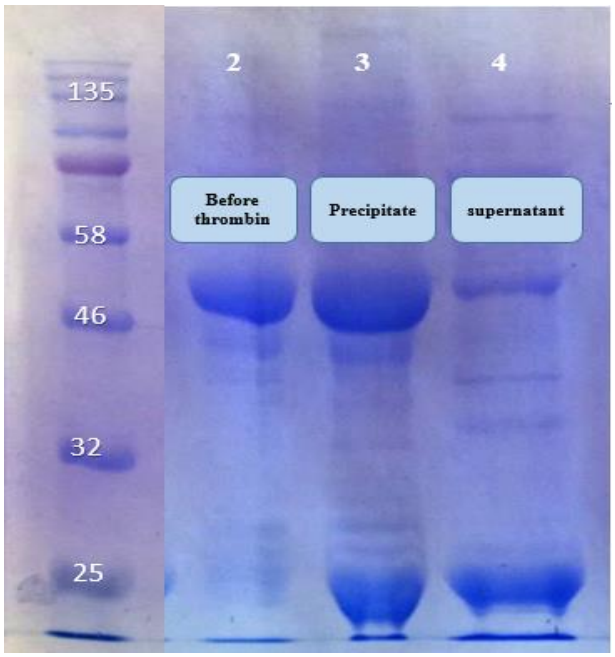

Figure 9: SDS-PAGE of the TSC2-218-N119K aggregation. Lane 1 is the molecular weight marker. Lane 2 is N119k-GST. Lane 3 is the aggregation. Lane 4 is the supernatant.

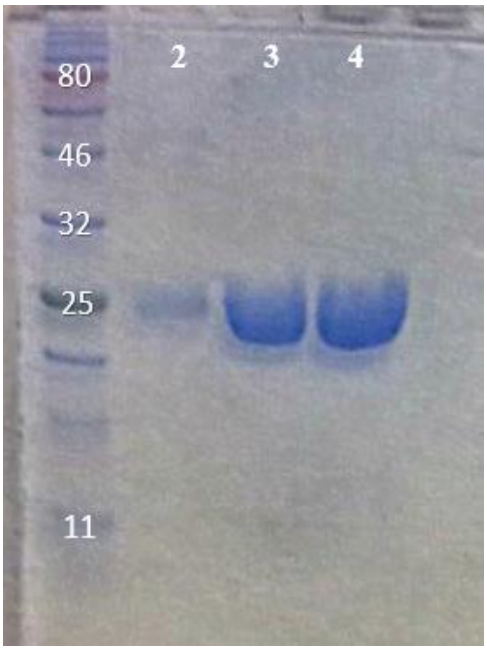

Figure 10b: SDS-PAGE of the concentrated TSC2-218 N119K. Lane 1 is the molecular weight marker. Lane 2, 3, 4 are protein fractions.

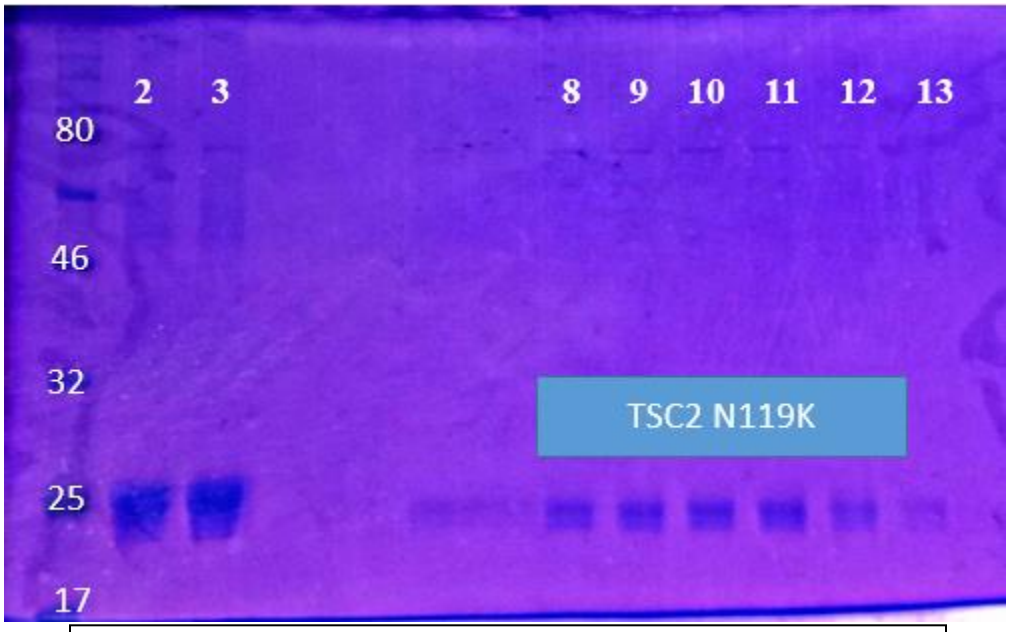

Figure 10a: SDS-PAGE of the N119K after the second affinity purification. Lane 1 is the molecular weight marker. Lane 2 and 3 are the cleaved protein. Lanes 8 - 13 are different fractions of the TSC2-218-N119K.

The Rheb GTPase domain was expressed as a His_6-tagged and purified as described in the previous section. An SDS-PAGE was applied to confirm the purity of the pooled fraction, which is shown in Figure 8. The presence of a very light band in the flow through indicated a successful attachment of the protein into the nickel column. The protein eluted at increasing concentration of imidazole and the bands were shown in Figure 11.

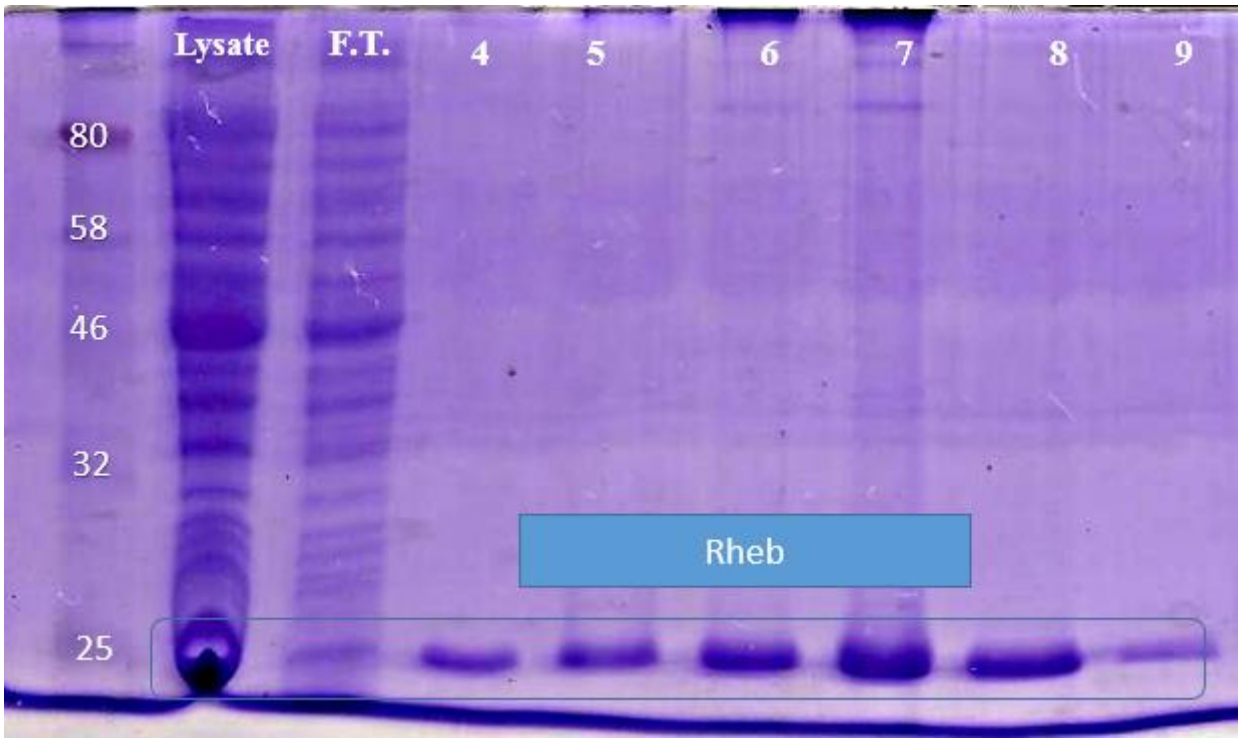

Figure 11: SDS-PAGE of Rheb after the affinity purification. Lane 1 is the molecular weight marker. Lane 2 is the lysate. Lane 3 is the flow through. Lanes 4 - 9 are different fractions of the protein.

3.3 Circular dichroism

To facilitate further analysis of the proteins' structural features, CD measurements were applied. CD spectra were obtained by monitoring the peaks at 190-250 nm and were compared to the typical spectra. Figure 12 shows the spectra of the wild type and the variant with two negative peaks at 211 nm. This observation confirmed that both proteins are composed mainly of alpha-helix structures. However, there was a slight difference between the spectra of the wild type and the variant, which suggested that the introduced mutation might have a slight effect on the protein structure.

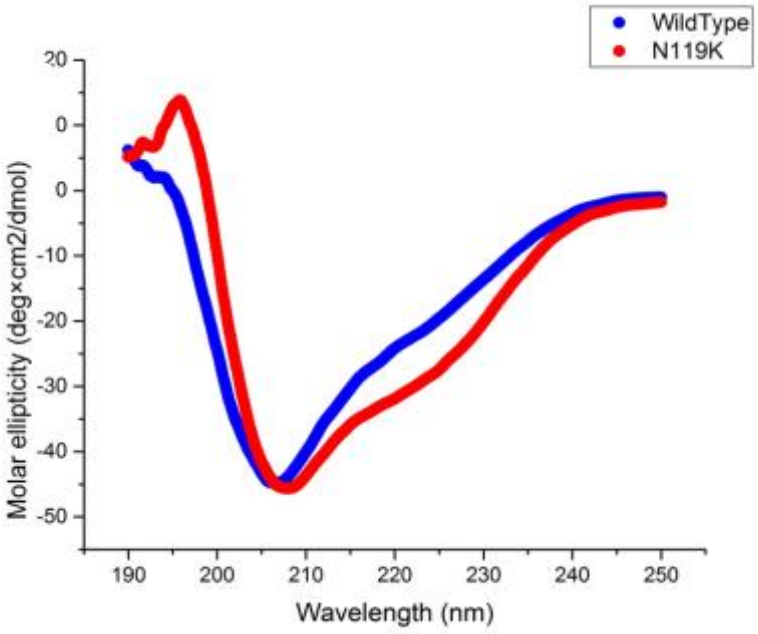

Figure 12: Native CD spectra of the wild type and the variant. The introduced signal-point mutation caused a slight change in the protein's secondary structure. The wild type is red and the variant is blue.

Difference spectra were recorded to visualize the effect of Rheb binding on the secondary structure in the TSC2-218 wild type and TSC2-218 (N119K). The CD spectra of the proteins were recorded in the far UV region (190-250 nm) (Figure 13a) The spectra were normalized and labelled in different colors: Blue is the unbound protein, orange is the protein bound to Rheb, and yellow is the bound protein subtracted from Rheb mathematically. For the TSC2-218 wild type, there was a change in the spectra for the unbound protein and the bound protein, and that indicated the conformational change of TSC2-128 wild type occurred because of Rheb binding. In addition, previous data highlight the fact that TSC2-218 binds to Rheb causing GTP hydrolysis using other applications such as GTP hydrolysis and NMR[29,30]. On the other hand, Figure 13b shows the difference spectra for the variant and displays a smaller difference between the bound and unbound TSC2-218 N119K than the TSC2-218 wild type. This finding signifies that the mutation causes a slight change on the protein secondary structure which may correlates with the binding between TSC2-218 (N119K) and Rheb. Further investigations using other biophysical techniques are necessary to confirm this finding.

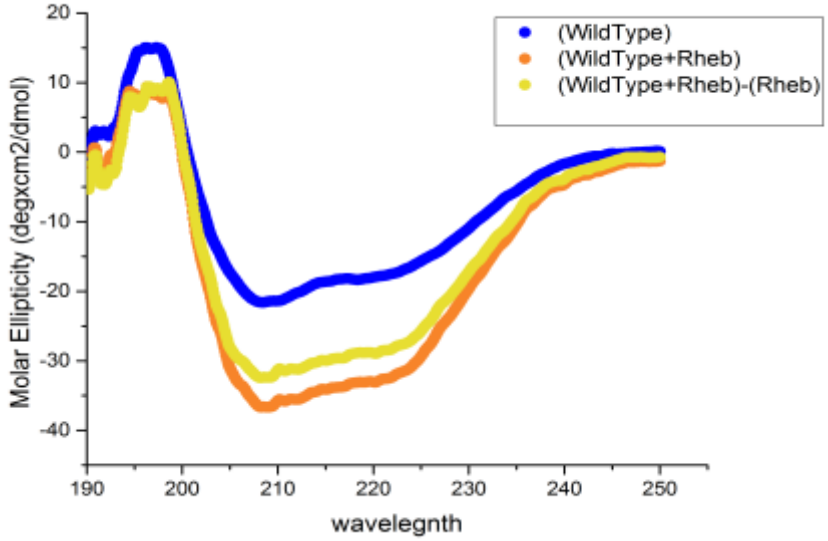

Figure 13a: CD Spectra of the wild type, wild type with Rheb, wild type without Rheb. Difference CD spectra of the wild type show a significant difference when it is bound to Rheb compared to unbound protein. The wild type is blue, wild type with Rheb is orange, wild type with Rheb subtracted from Rheb is yellow.

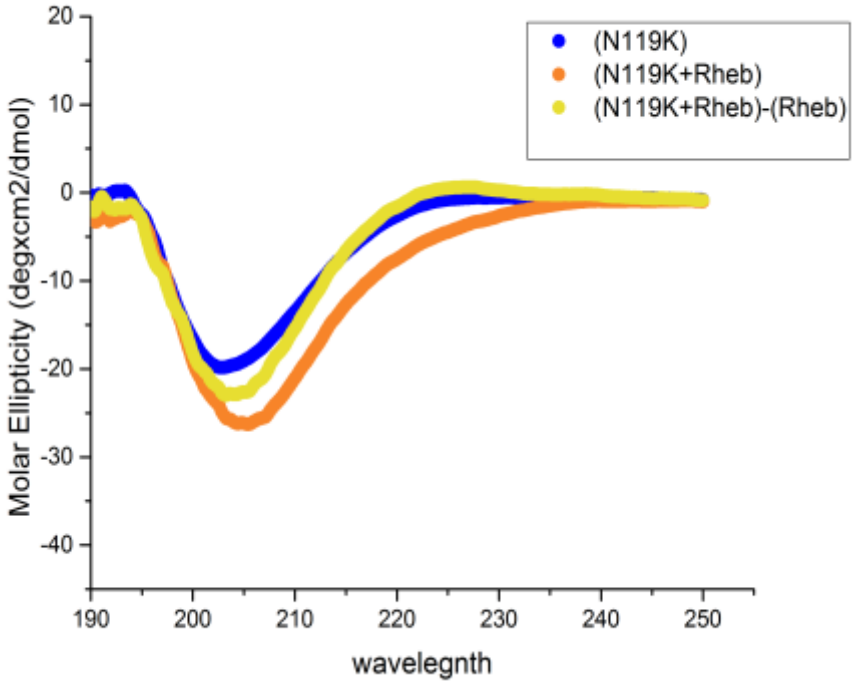

Figure 13b: CD Spectra of the variant, variant with Rheb, and variant without Rheb\. Difference CD spectrua of the variant show a minor difference when it is bound to Rheb compared to unbound one. The variant is blue, variant with Rheb is orange, and variant with Rheb subtracted from Rheb is yellow.

3.4 Thermal denaturation:

To assess the thermal stability of the wild type and the variant, thermal denaturation experiments were performed. Molar ellipticity values were monitored at 208 nm, which displayed the highest absolute values as can be seen in the negative peaks (Figure12). The melting temperatures of both proteins were calculated using the protein fraction denatured equation. Figure 14 presents the curves for thermal denaturation and shows the melting temperatures (Tm). The data shows that the calculated Tm for the wild type is 62° and for the variant is 64°. The similarity of the proteins' melting temperatures implies that the thermodynamic stability of the wild type was not significantly changed and reflects the slight difference shown in the CD spectra. As a result, the single point mutation N119K exhibits a low impact on the protein stability.

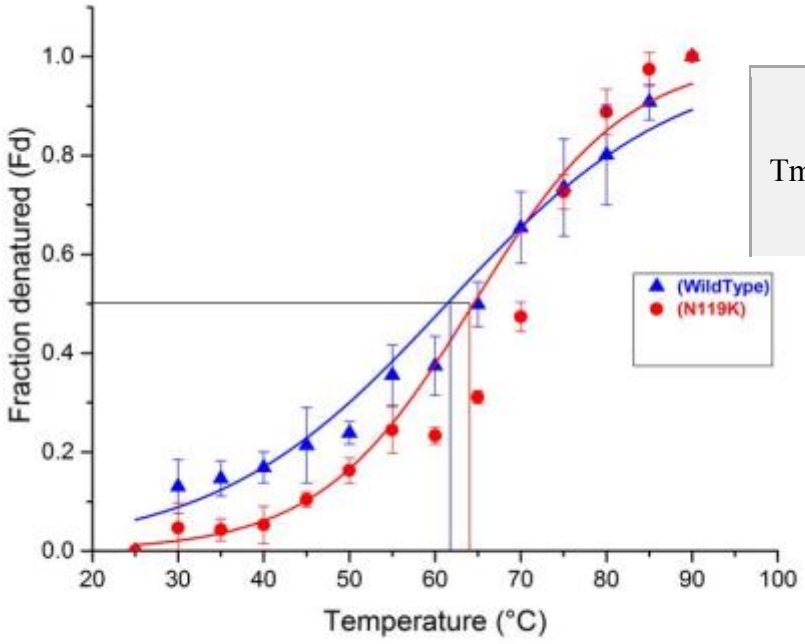

	WildType	Variant
Tm°	62°	64°

Figure 14: Thermal denaturation curves of the TSC2-218 wild type and variant. The introduced mutation did not change the melting temperature significantly. The wild type is blue and the variant is red.

3.5 Chemical denaturation:

Chemical denaturation was performed to measure the effect of the mutation on the protein stability under specific conditions. The stability measurements lay the groundwork for the variant characterization. The denaturation curves were generated by titrating increasing concentrations of 8 Molar (M) urea at 25°C. Urea disrupts the protein's secondary structure by breaking down the hydrogen bonds and allowing the hydrogen bonds binding to salts in order to stabilize the denatured protein. The intensity values were recorded by monitoring the fluorescence spectra at 340 nm (near UV region). As shown in Figure 12, at low concentration, the proteins barely started to unfold and they completely were denatured at less than 8 M concentration of urea. Both TSC2 wild type and variant contain two tryptophan residues (a major intrinsic flour) in the hydrophobic core and, as the urea concentration increased, the proteins started to unfold and that exposed the tryptophan residues to the surface, which showed more fluorescence intensity. The urea concentration, where the protein is half-unfolded (Cm), was calculated to be at 3.7 M for the TSC2-218 wild type and at 3.5 M urea for the variant N119K (Figure 15). This experiment revealed that both the wild type and the variant unfolded at the same concentration of urea. Therefore, the introduced mutation did not change the stability of the protein

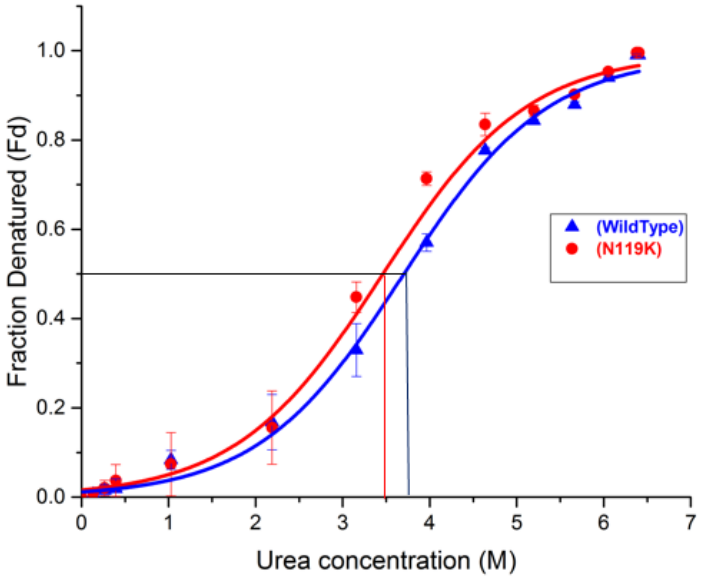

Cm	WildType	Variant
	3.7	3.5

Figure 15: Chemical denaturation curves of the TSC2-218 wild type and variant. The introduced mutation did not alter the chemical stability significantly. The wild type is blue and the variant is red.

Conclusion and future perspectives

4.1 Conclusion

The mTOR pathway is triggered by the active state of Rheb (Rheb-GTP). The activity of Rheb is partially controlled by TSC2 GAP domain that dephosphorylates Rheb-GTP and produces Rheb-GDP. Limited progress has been made in the investigation of TSC2-Rheb interaction, therefore, the molecular characterization of this interaction is not completely understood. In the study reported here, a single point mutation (N119K) in the GAP catalytic region is created to examine the importance of the asparagine residue. Several experiments were performed to study TSC2-218 N119K stability and interaction with Rheb.

The study of the structural properties provides insight into the variant activity. The thermal and chemical stability results strongly support that the variant could behave similarly to the wild type and that correlates to the similarity of the CD spectra. Although this study shows that Asn1643Lys mutation causes a minor change on the secondary structure in the presence of Rheb, an investigation of Rheb GTP hydrolysis using a quantitative technique is essential to analyze the variant GAP activity.

As stated before, it is believed that TSC2 GAP domain uses the Asn-thumb mechanism to stimulate Rheb GTP, which signifies the importance of this residue for catalysis[31]. A previous study shows the effect of Asn1643 mutation to several residues (including Ala, Asp, Gln, Arg, and Ile) on the GTPase activity of Rheb by obtaining ^{1}H, ^{15}N-HSQC-NMR spectra[32]. These mutations cause inhibition of the GAP activity towards Rheb, which underlie the cause of TSC disease. The dysfunction of the mutated GAP domain values the importance of the carboxylic-amide group[32]. Likewise, mutation of the residues in the GAP catalytic region of RAP1 GAP lead to activity hindrance[40,41]. However, it is unclear if theses mutations lose their activity

because of an absence or a weak binding. The investigation of the mutations binding will fill the gap in understanding the TSC2-Rheb interaction. Based on the other mutational studies, it is expected that Asn1643Lys might lose the activity to hydrolyze Rheb due it the absence of the carboxylic-amide group. However, this conclusion needs to be confirmed by applying additional experimentations.

4.2 Future perspectives:

This project has established the foundation of N119K characterization. Further studies of the N119K using nuclear magnetic resonance spectroscopy (NMR), ^{15}N Heteronuclear single quantum coherence (HSQC), will provide more knowledge about the residues that are responsible for the conformational changes. In addition, GTP hydrolysis will help to assess the ability of the variant to dephosphorylate Rheb and provide a quantitative measurement. For TSC2-218 N119K and Rheb binding, isothermal titration calorimetry (ITC) will be performed to examine the thermodynamic profile and the binding affinity to Rheb. A detailed study of the N119K variant will uncover more information about the variant's structure, activity and interaction.

The long-term objective is to provide more understanding into how TSC2 stimulates GTP hydrolysis of Rheb and how TSC2 regulates the mTOR pathway. This project's data and other TSC2 mutations findings will underline the causes of TSC disease. Moreover, the information may be used to develop more targeting areas for TSC therapeutic treatment.

References

1. Laplante M, Sabatini DM. mTOR signaling in growth control and disease. *Cell*. 2012. doi:10.1016/j.cell.2012.03.017.

2. Düvel K, Yecies JL, Menon S, et al. Activation of a metabolic gene regulatory network downstream of mTOR complex 1. *Mol Cell*. 2010. doi:10.1016/j.molcel.2010.06.022.

3. Ma XM, Blenis J. Molecular mechanisms of mTOR-mediated translational control. *Nat Rev Mol Cell Biol*. 2009. doi:10.1038/nrm2672.

4. Raught B, Peiretti F, Gingras A-C, et al. Phosphorylation of eucaryotic translation initiation factor 4B Ser422 is modulated by S6 kinases. *EMBO J*. 2004. doi:10.1038/sj.emboj.7600193.

5. Kim J, Kundu M, Viollet B, Guan K-L. AMPK and mTOR regulate autophagy through direct phosphorylation of Ulk1. *Nat Cell Biol*. 2011. doi:10.1038/ncb2152.

6. Dibble CC, Manning BD. Signal integration by mTORC1 coordinates nutrient input with biosynthetic output. *Nat Cell Biol*. 2013;15(6):555-564. doi:10.1038/ncb2763.

7. Yamagata K, Sanders LK, Kaufmann WE, et al. rheb, a growth factor- and synaptic activity-regulated gene, encodes a novel ras-related protein. *J Biol Chem*. 1994.

8. Im E, von Lintig FC, Chen J, et al. Rheb is in a high activation state and inhibits B-Raf kinase in mammalian cells. *Oncogene*. 2002. doi:10.1038/sj.onc.1205792.

9. Yu Y, Li S, Xu X, et al. Structural basis for the unique biological function of small GTPase RHEB. *J Biol Chem*. 2005;280(17):17093-17100. doi:10.1074/jbc.M501253200.

10. Karassek S, Berghaus C, Schwarten M, et al. Ras homolog enriched in brain (Rheb) enhances apoptotic signaling. *J Biol Chem*. 2010. doi:10.1074/jbc.M109.095968.

11. Mazhab-Jafari MT, Marshall CB, Ishiyama N, et al. An autoinhibited noncanonical mechanism of GTP hydrolysis by Rheb maintains mTORC1 homeostasis. *Structure*. 2012. doi:10.1016/j.str.2012.06.013.

12. Bai X, Ma D, Liu A, et al. Rheb activates mTOR by antagonizing its endogenous inhibitor, FKBP38. *Science*. 2007. doi:10.1126/science.1147379.

13. Ma D, Bai X, Guo S, Jiang Y. The switch I region of Rheb is critical for its interaction with FKBP38. *J Biol Chem*. 2008. doi:10.1074/jbc.M802356200.

14. Uhlenbrock K, Weiwad M, Wetzker R, Fischer G, Wittinghofer A, Rubio I. Reassessment of the role of FKBP38 in the Rheb/mTORC1 pathway. *FEBS Lett*. 2009. doi:10.1016/j.febslet.2009.02.015.

15. Wang X, Fonseca BD, Tang H, et al. Re-evaluating the roles of proposed modulators of mammalian target of rapamycin complex 1 (mTORC1) signaling. *J Biol Chem*. 2008. doi:10.1074/jbc.M803348200.

16. Shimobayashi M, Hall MN. Making new contacts: the mTOR network in metabolism and signalling crosstalk. *Nat Rev Mol Cell Biol*. 2014;15(3):155-162. doi:10.1038/nrm3757.

17. Sun Y, Fang Y, Yoon M-S, et al. Phospholipase D1 is an effector of Rheb in the mTOR pathway. *Proc Natl Acad Sci U S A*. 2008. doi:10.1073/pnas.0712268105.

18. Dibble CC, Elis W, Menon S, et al. TBC1D7 Is a Third Subunit of the TSC1-TSC2 Complex Upstream of mTORC1. *Mol Cell*. 2012. doi:10.1016/j.molcel.2012.06.009.

19. Henske EP, Scheithauer BW, Short MP, et al. Allelic loss is frequent in tuberous sclerosis kidney lesions but rare in brain lesions. *Am J Hum Genet*. 1996.

20. Van Slegtenhorst M, Nellist M, Nagelkerken B, et al. Interaction between hamartin and tuberin, the TSC1 and TSC2 gene products. *Hum Mol Genet*. 1998;7(6):1053-1057. doi:10.1093/hmg/7.6.1053.

21. Nakashima A, Yoshino K ichi, Miyamoto T, et al. Identification of TBC7 having TBC domain as a novel binding protein to TSC1-TSC2 complex. *Biochem Biophys Res Commun*. 2007. doi:10.1016/j.bbrc.2007.07.011.

22. Gai Z, Chu W, Deng W, et al. Structure of the TBC 1 D 7 – TSC 1 complex reveals that TBC 1 D 7 stabilizes dimerization of the TSC 1 C-terminal coiled coil region. 2016;0:1-15.

23. Plank TL, Logginidou H, Klein-Szanto A, Henske EP. The expression of hamartin, the product of the TSC1 gene, in normal human tissues and in TSC1- and TSC2-linked angiomyolipomas. *Mod Pathol*. 1999.

24. Potter CJ, Huang H, Xu T. Drosophila Tsc1 functions with Tsc2 to antagonize insulin signaling in regulating cell growth, cell proliferation, and organ size. *Cell*. 2001. doi:10.1016/S0092-8674(01)00333-6.

25. Tapon N, Ito N, Dickson BJ, Treisman J, Hariharan I. The Drosophila tuberous sclerosis complex gene homologs restrict cell growth and cell proliferation. *Cell*. 2001.

26. European Chromosome 16 Tuberous Sclerosis Consortium. Identification and characterization of the tuberous sclerosis gene on chromosome 16. *Cell*. 1993;75(7):1305-1315. doi:0092-8674(93)90618-Z [pii].

27. Maheshwar MM, Cheadle JP, Jones AC, et al. The GAP-related domain of tuberin, the product of the TSC2 gene, is a target for missense mutations in tuberous sclerosis. *Hum*

Mol Genet. 1997;6(11):1991-1996. doi:10.1093/hmg/6.11.1991.

28. Maheshwar MM, Cheadle JP, Jones AC, et al. The GAP-related domain of tuberin, the product of the TSC2 gene, is a target for missense mutations in tuberous sclerosis. *Hum Mol Genet*. 1997. doi:10.1093/hmg/6.11.1991.

29. Barnes MR, Gray IC. *Bioinformatics for Geneticists*.; 2003. doi:10.1007/s10549-011-1934-z.

30. Albert LL, Lehninger AL. *Lehninger Principles of Biochemistry / David L. Nelson, Michael M. Cox*.; 2005.

31. Resat H, Straatsma TP, Dixon D a, Miller JH. The arginine finger of RasGAP helps Gln-61 align the nucleophilic water in GAP-stimulated hydrolysis of GTP. *Proc Natl Acad Sci U S A*. 2001. doi:10.1073/pnas.091506998.

32. Marshall CB, Ho J, Buerger C, et al. Characterization of the Intrinsic and TSC2-GAP-Regulated GTPase Activity of Rheb by Real-Time NMR. *Sci Signal*. 2009. doi:10.1126/scisignal.2000029.

33. Biochemical and Biophysical Studies of Novel Features of Ras-related Protein Interactions.

34. Castro AF, Rebhun JF, Clark GJ, Quilliam LA. Rheb binds tuberous sclerosis complex 2 (TSC2) and promotes S6 kinase activation in a rapamycin- and farnesylation-dependent manner. *J Biol Chem*. 2003. doi:10.1074/jbc.C300226200.

35. Dieffenback Tmj ^P Dueksler, Gs E ^P L. General concepts for PCR primer design. *PCR Methods Appl*. 1993:30-87. doi:10.1101/gr.3.3.S30.

36. Lee SY, Zhang Y, Skolnick J. TASSER-based refinement of NMR structures. *Proteins Struct Funct Genet*. 2006. doi:10.1002/prot.20902.

37. Guide QR. UCSF Chimera. *Search*. 2007. doi:10.1016/j.jsb.2011.09.006.

38. Greenfield NJ. Using circular dichroism spectra to estimate protein secondary structure. *Nat Protoc*. 2006. doi:10.1038/nprot.2006.202.

39. Harper S, Speicher DW. Purification of proteins fused to glutathione S-transferase. TL - 681. *Methods Mol Biol*. 2011. doi:10.1007/978-1-60761-913-0_14.

40. Scrima A, Thomas C, Deaconescu D, Wittinghofer A. The Rap-RapGAP complex: GTP hydrolysis without catalytic glutamine and arginine residues. *EMBO J*. 2008. doi:10.1038/emboj.2008.30.

41. Daumke O, Weyand M, Chakrabarti PP, Vetter IR, Wittinghofer A. The GTPase-

activating protein Rap1GAP uses a catalytic asparagine. *Nature*. 2004. doi:10.1038/nature02505.

42. RCSB. Research Collaboratory for Structural Bioinformatics (RCSB). http://www.rcsb.org/pdb/home/home.do.